Journal of Catalysis 263 (2009) 277–283

Contents lists available at ScienceDirect

Journal of Catalysis

www.elsevier.com/locate/jcat

# Effect of pore size and acidity on the coke formation during ethylbenzene conversion on zeolite catalysts

Jun Huang, Yijiao Jiang, V.R. Reddy Marthala, Arne Bressel, Joerg Frey, Michael Hunger *

*Institute of Chemical Technology, University of Stuttgart, 70550 Stuttgart, Germany*

ARTICLE INFO

*Article history:*
Received 1 September 2008
Revised 26 January 2009
Accepted 14 February 2009
Available online 4 March 2009

*Keywords:*
Ethylbenzene disproportionation
Coke formation
Acidic zeolites
Pore size
Transition state shape selectivity
*In situ* solid-state NMR spectroscopy

ABSTRACT

The present work provides solid-state $^{13}C$ NMR spectroscopic evidence that the zeolites acidity and the pore size strongly affect the catalytic behavior of ethylbenzene disproportionation and coke formation. The medium-pore zeolite H-ZSM-5 (*ca.* 0.56 nm) and the large-pore zeolite H-Y (*ca.* 0.74 nm) used in this study have exclusively Brønsted acid sites, but with different acid strength. Due to the transition state shape selectivity of ethylbenzene disproportionation, ethylbenzene transalkylation on H-Y takes place at low reaction temperature without side-reactions. On H-ZSM-5, dealkylation/realkylation was observed and generation of alkylcarbenium ions resulted in secondary reactions. These alkylcarbenium ions initiate coke formation on zeolite H-ZSM-5 *via* oligomerization, six-ring closure, and aromatization of alicyclic hydrocarbons. Ethylbenzene disproportionation on large-pore zeolites Y is an attractive reaction due to its low reaction temperature, high selectivity without side-reactions, and low coke formation. Medium-pore zeolite H-ZSM-5 showed higher reactivity for dealkylation of ethylbenzene and protolytic cracking of light alkanes due to its narrow channels and stronger Brønsted acid sites.



## 1. Introduction

Disproportionation of aromatic hydrocarbons is an important acid catalyzed petrochemical reaction [1,2]. Ethylbenzene disproportionation into benzene and diethylbenzene has not been commercialized until recently [3]. But it has been studied extensively, because *p*-diethylbenzene has a high industrial potential in the recovery of *p*-xylene in the Parex and Eluxyl process [4]. Till now, most of the mechanistic studies of ethylbenzene disproportionation have been carried out with liquid Friedel–Crafts or superacidic catalysts [5–7]. Two main reaction pathways were proposed: (i) The diphenylethane-mediated reaction pathway (Scheme 1) and (ii) the ethyl-transfer reaction pathway (Scheme 2).

On the basis of H/D exchange and $^{14}C$-label transfer experiments between ethylbenzene and $\alpha$-ethylphenyl cations in a solution of benzene containing gallium and hydrogen bromide, a reaction pathway involving the diphenylethane species and the mechanistic cycle in Scheme 1 were proposed [2,5]. It was found that ethylbenzene molecules react with $\alpha$-ethylphenyl cations to form diphenylethane species, which are further split into benzene and an $\alpha$-diethylphenyl cation. After hydride transfer between the $\alpha$-diethylphenyl cation and a second ethylbenzene, diethylbenzene is produced with the generation of a new $\alpha$-ethylphenyl cation. It promotes the reaction in the catalytic cycle. The hydride transfer was considered as the rate determining step of the reaction [5].

Mechanistic studies of alkyl group transfer in the alkylbenzene disproportionation have been firstly carried out in liquid acids prepared by a mixture of hydrogen fluoride and boron trifluoride [6]. According to these investigations, the alkyl group maintains its configuration while transferring from one ring to the other at room temperature *via* a transition state containing a partial bond between the alkyl group and a second alkylbenzene. The experimental results showed that ethylbenzene was disproportionated to *ca.* 90% *via* this pathway at room temperature [6]. However, the protonated alkylbenzene was split into a benzene molecule and an alkylcarbenium ion at higher temperatures (439 to 553 K) as shown in Scheme 2. This carbenium ion alkylated a second alkylbenzene to complete the disproportionation [2,6]. At the same time, some highly reactive alkylcarbenium ions react further by polymerization or hydride abstraction. The experiments demonstrated that the alkylbenzene disproportionation by this mechanism is accompanied by side-reactions leading to complex products [6]. The migration of methyl groups in xylene was found to be much slower than that of ethyl groups in ethylbenzene [7]. In a solution of excess HF-$BF_3$, no conversion of xylenes occurred at 339 K, but the ethylbenzene almost completely disproportionated at 273 K [7].

Zeolites are solid acids and considered as one kind of efficient, safe, and environmentally benign catalysts to replace liquid acids in chemical industry [1]. Therefore, zeolites are used as important catalysts in hydrocarbon chemistry [1]. In comparison to liquid

* Corresponding author. Fax: +49 711 685 64081.
*E-mail address:* michael.hunger@itc.uni-stuttgart.de (M. Hunger).

0021-9517/$ – see front matter 
doi:10.1016/j.jcat.2009.02.019

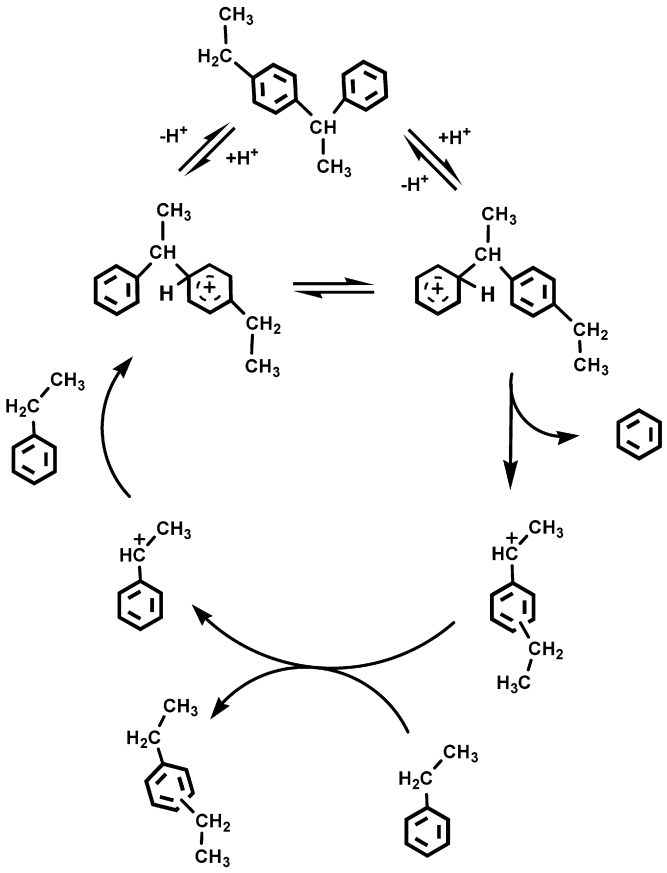

Scheme 1.

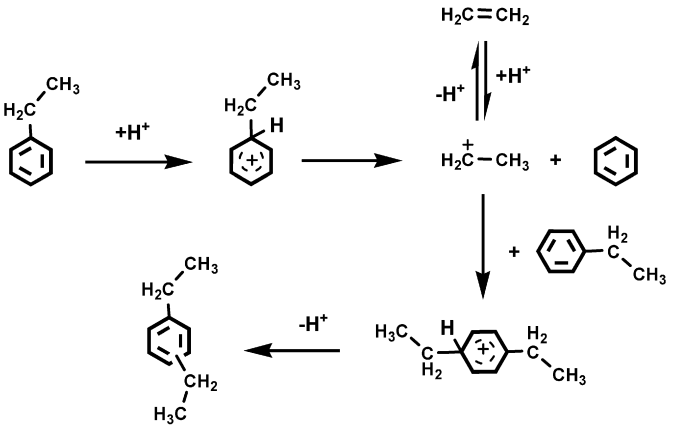

Scheme 2.

acids, however, the chemical environment for ethylbenzene disproportionation on zeolites are totally other, which is caused not only by the distribution of acid sites and their properties, but also by the shape selectivity of these microporous materials [1]. After a sufficiently long time-on-stream, the rate of the ethylbenzene disproportionation is virtually constant and can be correlated with the concentration of strong Brønsted acid sites on zeolite catalysts [8–14]. Therefore, ethylbenzene disproportionation was further suggested by the Catalysis Commission of the International Zeolite Association (IZA) as a test reaction for acidic zeolite catalysts [15]. In addition, this reaction is a shape selective reaction on zeolites. The reaction shows an induction period on large-pore zeolites and no induction period on medium-pore zeolites [8–14].

The present work describes *in situ* solid-state $^{13}C$ NMR investigations of the ethylbenzene conversion on large-pore zeolite H-Y and medium-pore zeolite H-ZSM-5 containing exclusively Brønsted acid sites. These zeolites have different acid strength and both are widely used commercial catalysts in the petrochemical industry. The study gives new insights how the acid strength and pore size of zeolites influence the coke formation on these catalysts.

Large organic compounds formed *via* hydrocarbon reactions could be trapped in the cages of acidic zeolite catalysts, which always results in a catalyst deactivation under reaction conditions [16]. Therefore, understanding of coke formation is an important economical objective for the industrial application of these types of catalysts. Solid-state NMR spectroscopy is acting as an advanced method to monitor hydrocarbon reactions inside the zeolite pores with high resolution and sensitivity due to its non-destructive nature [17]. In this study, ethylbenzene reactions (including disproportionation, side-reaction, and coke formation) on zeolites H-Y and H-ZSM-5 were investigated by *in situ* solid-state $^{13}C$ NMR spectroscopy. Different organic compounds were identified inside the zeolite pores at intermediate stages of the catalytic reaction, providing information for understanding the reaction and deactivation mechanisms.

## 2. Experimental

Zeolites H-Y ($n_{Si}/n_{Si} = 2.7$) and H-ZSM-5 ($n_{Si}/n_{Si} = 26$) were prepared as described in Ref. [18]. All zeolite catalysts were characterized by XRD and $^{27}Al$ and $^{29}Si$ MAS NMR spectroscopy, indicating that the obtained materials were neither damaged nor dealuminated. By quantitative $^{1}H$ MAS NMR measurements, the concentration of Brønsted acid sites (SiOHAl groups) located in the supercages of zeolite H-Y and in the channels of zeolite H-ZSM-5 was determined to 1.72 and 0.42 mmol/g, respectively.

For the present study, the zeolites were filled into a glass tube and subjected to activation in vacuum with the heating rate of 20 K/h up to the final temperature of 723 K. At this temperature, the zeolites were evacuated to below $10^{-2}$ mbar for 12 h. Then, $^{13}C$-enriched ethyl[$\alpha$-$^{13}C$]benzene ($^{13}C$-enrichment of 99%, purchased from Dr. Ehrenstorfer) was quantitatively loaded, *i.e.*, 1 molecule per accessible SiOHAl group in zeolites H-Y and H-ZSM-5, which corresponds to 2 molecules per supercage of zeolite H-Y. Subsequently, these samples were sealed in glass tubes. The heating of the sealed samples was performed in an external oven, while the solid-state NMR studies were carried out at room temperature.

All $^{13}C$ MAS NMR investigations were performed with a 7 mm Bruker MAS NMR probe on a Bruker MSL-400 spectrometer at the resonance frequency of 100.6 MHz. $^{13}C$ high-power proton decoupling (HPDEC) MAS NMR spectra were recorded after an excitation with a $\pi/2$ pulse and with the repetition time of 5 s. $^{13}C$ cross-polarization (CP) MAS NMR spectra were recorded with the contact time of 5 ms and the repetition time of 2 s. Sample spinning rates of *ca.* 4 kHz were applied. All solid-state $^{13}C$ NMR spectra were referenced to tetramethylsilane (TMS).

## 3. Results

### 3.1. Ethylbenzene conversion on zeolites H-Y and H-ZSM-5 at 298 to 503 K

Solid-state $^{13}C$ NMR spectroscopy was utilized to demonstrate the progression of the ethylbenzene reaction on zeolites at different temperatures. Figs. 1 and 2 show the $^{13}C$ CP MAS NMR spectra of ethylbenzene adsorption and conversion on zeolites H-Y and H-ZSM-5 at 298, 453, and 503 K. Before the first heating, a dominating peak at 29 ppm occurs in spectra due to the $^{13}C$-enriched

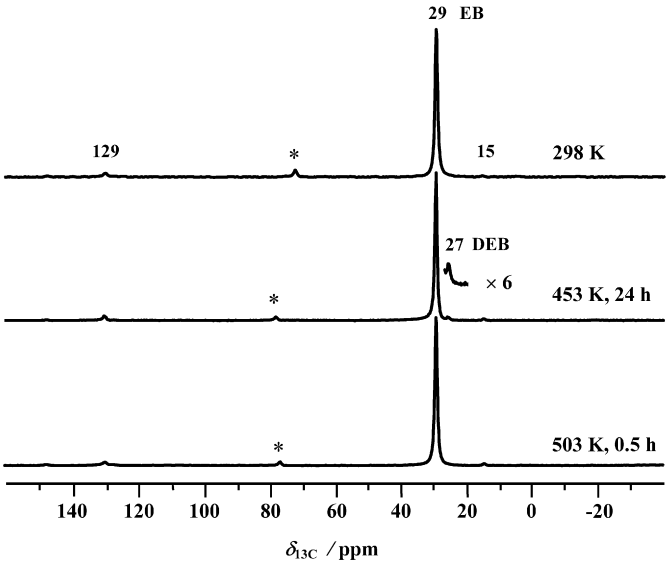


**Fig. 1.** $^{13}$C CP MAS NMR spectra of ethyl[$\alpha$-$^{13}$C]benzene conversion on zeolite H-Y (1 molecule per accessible SiOHAl group) at 298 to 503 K. Asterisks denote spinning sidebands.

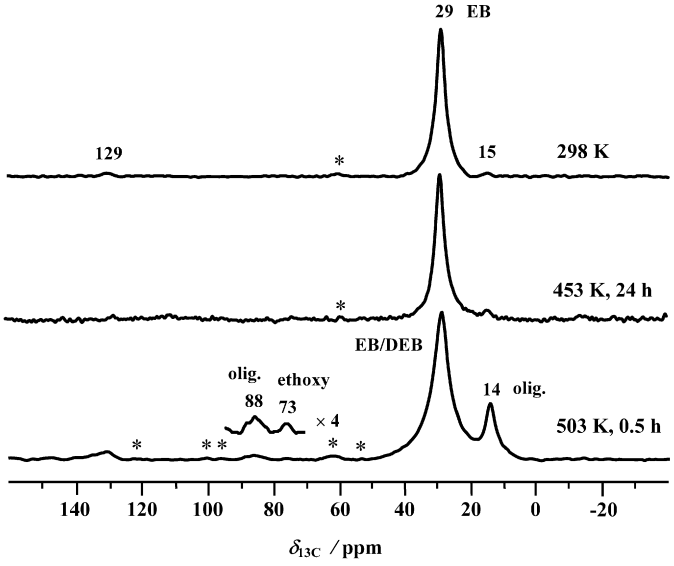


**Fig. 2.** $^{13}$C CP MAS NMR spectra of ethyl[$\alpha$-$^{13}$C]benzene conversion on zeolite H-ZSM-5 (1 molecule per SiOHAl group) at 298 to 503 K. Asterisks denote spinning sidebands.

methylene group in the side-chain of ethylbenzene [19]. Two weak signals at 15 and 129 ppm are assigned to the non-enriched carbon atoms at the methyl group and the aromatic ring. No conversion of ethylbenzene was observed at 298 K.

Upon heating of zeolite H-Y at 453 K for 24 h, a new $^{13}$C MAS NMR signal occurred at 27 ppm (Fig. 1) due to the formation of diethylbenzene. Treating of zeolite H-ZSM-5 under the same conditions did not result in the conversion of ethylbenzene (Fig. 2). At 503 K, the ethylbenzene is converted within a short time (0.5 h). Already earlier studies indicated that ethylbenzene disproportionation on large-pore zeolites Y requires long reaction times at low reaction temperature, while this reaction on medium-pore zeolites needs higher temperature [1,8–14]. A strong signal at 14 ppm and two weak signals at 73 and 88 ppm occurred in the $^{13}$C CP MAS NMR spectra of zeolite H-ZSM-5 (Fig. 2, bottom). The signal at 73 ppm can be assigned to surface $^{13}$C-1-ethoxy groups according to their formation on zeolite Y after adsorption of $^{13}$C-1-ethanol

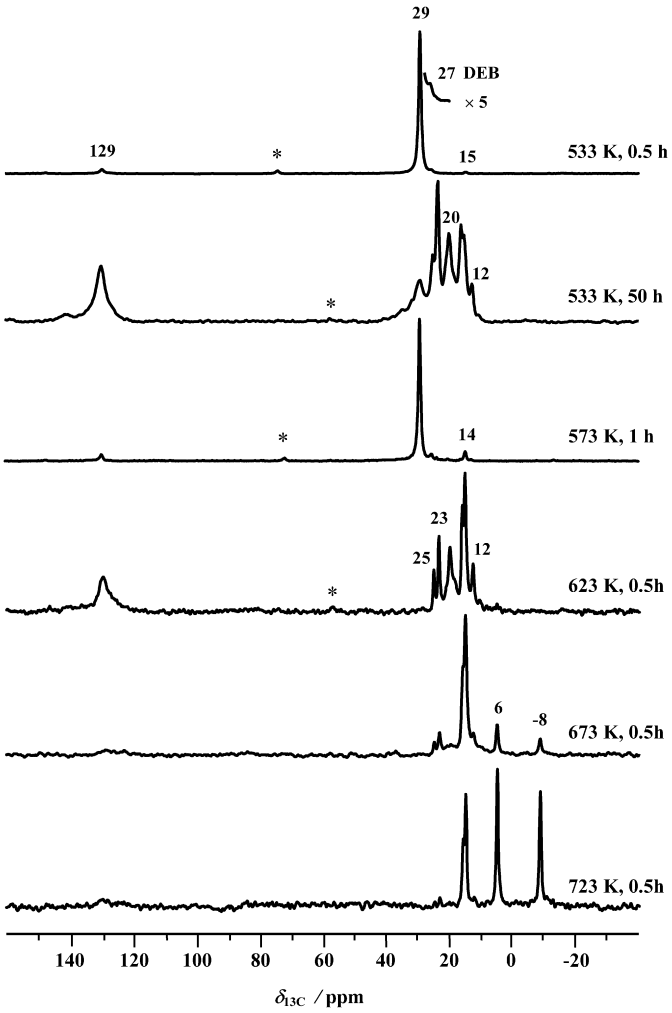


**Fig. 3.** $^{13}$C HPDEC MAS NMR spectra of ethyl[$\alpha$-$^{13}$C]benzene conversion on zeolite H-Y (1 molecule per accessible SiOHAl group) at 533 to 723 K. Asterisks denote spinning sidebands.

at 453 K [20]. This active surface species can react with a second ethylbenzene molecule to form diethylbenzene. Upon decomposition of surface $^{13}$C-1-ethoxy species at 523 K, Wang et al. [20] observed a weak and broad signal at 78 to 89 ppm and a strong signal at 13 ppm. In a similar manner, Stepanov et al. [21] assigned the signals at 89 ppm and 14 ppm obtained after adsorption of $^{13}$C-1-ethylene on H-ZSM-5 at 296 K to oligomeric alkoxy groups and terminal methyl carbons of these alkoxy species, respectively.

### *3.2. Ethylbenzene conversion on zeolites H-Y and H-ZSM-5 at 533 to 723 K*

When heating the ethylbenzene-loaded zeolites H-Y and H-ZSM-5 at 533 to 723 K, the ethylbenzene reaction is complex (Figs. 3 and 4). At 533 K, the ethylbenzene conversion on zeolite H-Y starts in 0.5 h and produces exclusively diethylbenzene, which results in a weak $^{13}$C MAS NMR signal at 27 ppm (Fig. 3). Since no signals of by-products occur, the ethylbenzene conversion goes along the bimolecular pathway *via* diphenylethane-type intermediate. A former H/D exchange study on acidic zeolite Y performed using *in situ* pulsed-flow $^{1}$H MAS NMR spectroscopy also demonstrated that the C–H bond at side chain of ethylbenzene can be activated at 523 K within 5 minutes [22]. This finding indicates that heating temperatures of higher than 503 K promote the ethylbenzene disproportionation and decrease the reaction time.

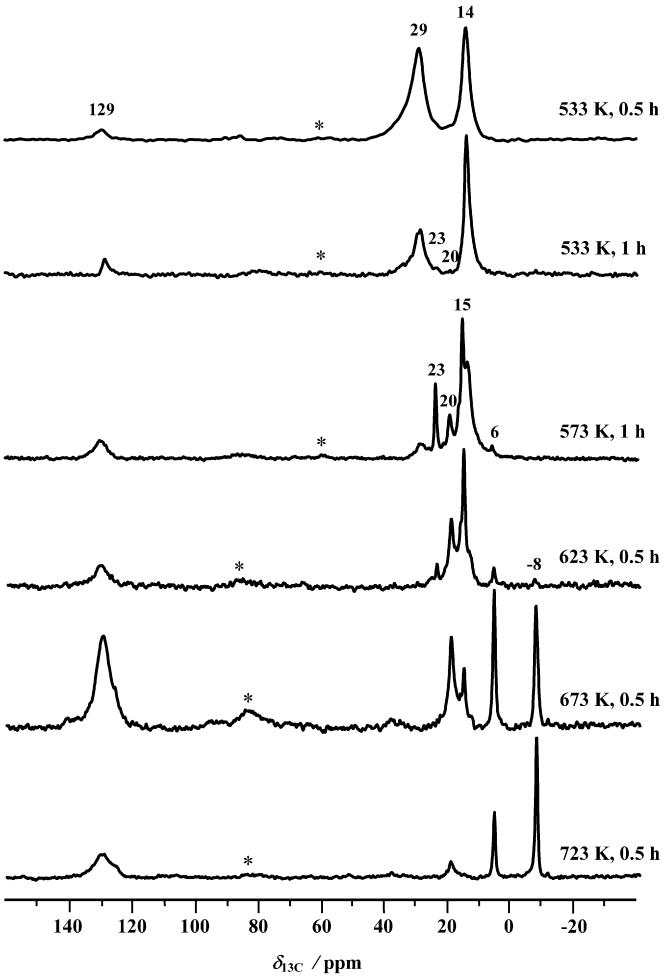


**Fig. 4.** $^{13}$C HPDEC MAS NMR spectra of ethyl[$\alpha$-$^{13}$C]benzene conversion on zeolite H-ZSM-5 (1 molecule per SiOHAl group) at 533 to 723 K. Asterisks denote spinning sidebands.

As indicated by the spectra in Fig. 3, however, further increase of the reaction temperature or prolongation of the reaction time promote the formation of protonated diethylbenzene or ethylbenzene cations, which reach the activation energy for the dealkylation of the ethyl groups under these conditions. The obtained ethyl cations are deprotonated to ethylene or cause further side-reactions. After heating zeolite H-Y at 533 K for 50 h or at 573 K for 1 h, the ethyl cations are involved in oligomerization, hydride transfer, and aromatization reactions. These reactions cause new products, which are observed in the $^{13}$C HPDEC MAS NMR spectra as signals of methyl groups of oligomeric alkoxy species at 14 ppm, butane at 23 ppm, propane at 15 ppm, toluene at 129 and 20 ppm, and other aromatic compounds at 129 ppm. Compared to zeolite H-Y, the zeolite H-ZSM-5 shows a higher reactivity in the ethylbenzene dealkylation. On zeolite H-ZSM-5, oligomeric alkoxy species were already produced at 503 K (Fig. 2), while the formation of these compounds on zeolite H-Y require heating at 533 K. Bhan and Iglesia [23] concluded that smaller zeolite pores enhance the catalytic reactivity. Therefore, the high activity of zeolite H-ZSM-5 in the ethylbenzene dealkylation may have two reasons: strong Brønsted acid sites and small pores.

As shown in Fig. 4, the $^{13}$C MAS NMR signal at 14 ppm caused by methyl groups of oligomeric species is strongly increased upon heating at 533 K with the expanse of the peak of *p*-diethylbenzene and ethylbenzene at 29 ppm. Due to the shape selective behavior of the medium-pore zeolite H-ZSM-5, *p*-diethylbenzene, which is

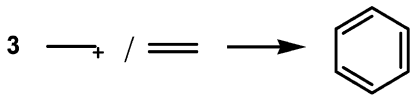


**Scheme 3.**

characterized by the $^{13}$C MAS NMR shift of 28.8 ppm, is the most preferred product of the ethylbenzene disproportionation and is responsible for the broadening of the signal at *ca.* 29 ppm [1]. In this case, the intensity of the signal of aromatics at 129 ppm is increasing slowly, which indicates that the direct aromatization of ethyl cations or ethylene molecules according to Scheme 3 is hindered. This phenomenon was also observed for the ethylbenzene conversion on zeolite H-MOR [19]. Therefore, the ethyl cations and ethylene molecules are promoted to realkylate ethylbenzene or to oligomerize. Upon expanding the heating time to 1 h, most of the $^{13}$C-enriched ethyl groups were dealkylated from diethylbenzene and ethylbenzene and converted to oligomeric species. When increasing the heating temperature of the ethylbenzene-loaded zeolite H-ZSM-5 to 573 K, the intensity of the signal at 14 ppm, due to methyl groups bound to oligomeric alkoxy species, was decreased and the intensity of the signal at 129 ppm, due to aromatic compounds, was obviously increased accompanied by the appearance of new signals at 6, 15, 20, and 23 ppm (ethane, propane, toluene, and butane, respectively). This phenomenon also occurred for the ethylbenzene conversion on zeolite H-Y at 533 K for 50 h and at 623 K for 0.5 h (Fig. 3).

The $^{13}$C MAS NMR spectra obtained for the ethylbenzene conversion on zeolite H-Y at 533 to 623 K obviously consist of two additional signals at 12 and 25 ppm (Fig. 3) in comparison with the spectra of ethylbenzene-loaded zeolite H-ZSM-5 (Fig. 4). In the case of zeolite H-ZSM-5 heated at 623 K, the $^{13}$C MAS NMR signal of methane at −8 ppm starts to appear (Fig. 4). In the case of zeolite H-Y, the formation of methane requires heating at 673 K. This finding indicates that for the zeolite catalysts under study the hydrocarbon cracking takes place at the above-mentioned temperatures. Upon raising the reaction temperature up to 723 K, the intensity of signals due to ethane and methane at 6 ppm and −8 ppm, respectively, are increased accompanied by a decrease of the signal of propane at 15 ppm.

Heating of ethylbenzene-loaded zeolite H-Y at 673 and 723 K leads to a significant decrease of the $^{13}$C HPDEC MAS NMR signals of aromatics at 129 ppm (Fig. 3). In contrast, the $^{13}$C CP MAS NMR spectra of this sample (Fig. 5) still showed broad signals at 120 to 140 ppm due to the presence of non-substituted aromatics (120–130 ppm) and alkyl-substituted aromatics (135–140 ppm) [24]. In the case of zeolite H-ZSM-5 heated at 673 and 723 K, however, both $^{13}$C HPDEC and $^{13}$C CP MAS NMR spectra (Figs. 4 and 6, respectively) contain strong signals of aromatic compounds and the intensity of these signals decreases only slightly with increasing reaction temperature. Hence, the amount of coke deposits is significantly larger on zeolite H-ZSM-5 than on H-Y under same reaction conditions.

## 4. Discussion

### *4.1. Mechanisms of the ethylbenzene disproportionation on zeolites H-Y and H-ZSM-5*

In the present work, medium-pore zeolite H-ZSM-5 (*ca.* 0.56 nm) and large-pore zeolite H-Y (*ca.* 0.74 nm) containing exclusively Brønsted acid sites were utilized as catalysts for *in situ* $^{13}$C MAS NMR investigations of the ethylbenzene conversion. As evidenced by adsorption of the weak base acetonitrile as a probe molecule, the Brønsted acid sites of zeolite H-ZSM-5 are characterized by a higher acid strength than those of zeolite H-Y [18]. In the

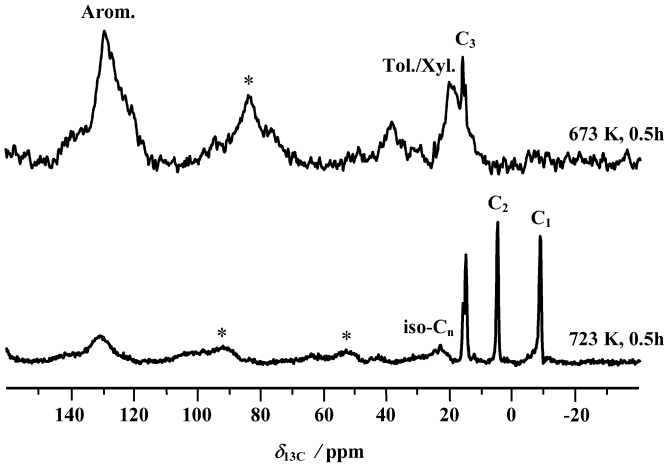


**Fig. 5.** $^{13}$C CP MAS NMR spectra of ethyl[$\alpha$-$^{13}$C]benzene conversion on zeolite H-Y (1 molecule per accessible SiOHAl group) at 673 and 723 K. Asterisks denote spinning sidebands.

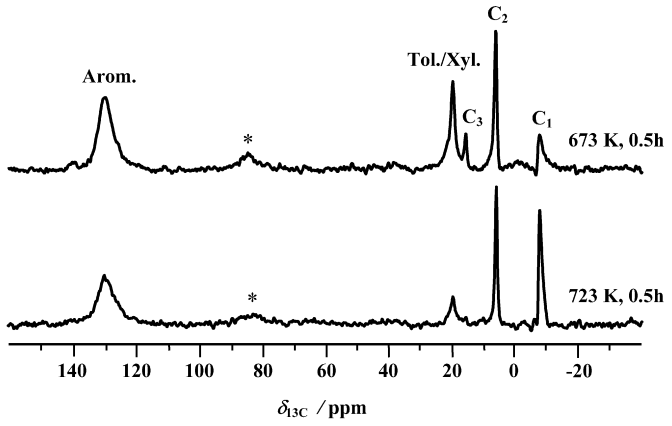


**Fig. 6.** $^{13}$C CP MAS NMR spectra of ethyl[$\alpha$-$^{13}$C]benzene conversion on zeolite H-ZSM-5 (1 molecule per SiOHAl group) at 673 and 723 K. Asterisks denote spinning sidebands.

above-mentioned $^{1}$H MAS NMR studies, adsorbate-induced low-field shifts $\Delta\delta_{1H}$ of 5.1 and 7.9 ppm were obtained for acetonitrile-loaded zeolites H-Y and H-ZSM-5, respectively [18]. Acetonitrile applied as probe molecule for acidic zeolites interacts *via* hydrogen bonding with the Brønsted acid sites. In this case, a higher low-field shift corresponds to a higher acid strength and *vice versa*. In addition, the small pore size of zeolite H-ZSM-5 should enhance the interaction between reactants and active surface sites [23,25], which promotes the reaction. Assuming same pathways for the ethylbenzene conversion on zeolites H-Y and H-ZSM-5, therefore, the reaction rate should be higher on zeolite H-ZSM-5 than on zeolite H-Y and diethylbenzene should be produced at 453 K on both catalysts. However, former studies and the present work did not show any ethylbenzene disproportionation at 453 K on zeolite H-ZSM-5. In agreement with earlier studies ([1] and references therein), therefore, it must be assumed that the reaction mechanisms of the ethylbenzene disproportionation are different on medium-pore zeolite H-ZSM-5 and large-pore zeolite H-Y.

Generally, it is accepted that ethylbenzene disproportionation on large-pore zeolites proceeds *via* diphenylethane species as intermediates (Scheme 1). The generation of $\alpha$-ethylphenyl cations is very important for this reaction mechanism, because the catalytic cycle is initiated by this cation. Quantum-chemical calculations indicated that acidic zeolites can start the transalkylation of *m*-xylene by a hydride abstraction to form a carbenium ion at one of the methyl groups with the activation energy of 206 kJ/mol [26]. According to recent *in situ* pulsed-flow $^{1}$H MAS NMR spectroscopic investigations [22], the initial C–H bond activation at the side chain of ethylbenzene and the formation of carbenium ions on zeolite H-Y requires higher reaction temperatures or longer heating time. This explains also the effect of the long reaction time for the ethylbenzene disproportionation on zeolite H-Y (Fig. 1).

The occurrence of signals due to ethoxy groups in the $^{13}$C MAS NMR spectra in Fig. 2 indicates that the ethylbenzene disproportionation on the medium-pore zeolite H-ZSM-5 is a monomolecular reaction *via* the ethoxy-mediated pathway (Scheme 2). After adsorption of ethylbenzene on zeolites, the aromatic ring is rapidly protonated to form the ethylcyclohexadienyl carbenium ion. At higher temperatures, this cation is dealkylated to an ethyl cation and a benzene molecule. The alkyl cation is stabilized by a nearby zeolite $SiO^{-}Al$ site to the more stable ethoxy group or decomposed to ethylene. Furthermore, the alkyl cation can contact a second ethylbenzene to yield diethylbenzene. In addition, ethylene can be transformed subsequently to oligomeric alkoxy species by fast oligomerization [21]. This side-reaction was also observed for the ethylbenzene disproportionation in a solution of HF-$BF_3$ and is considered as a hint to the monomolecular reaction mechanism [6]. On zeolite H-Y, however, exclusively diethylbenzene and benzene are formed in result of the ethylbenzene disproportionation at low reaction temperatures as indicated by the corresponding $^{13}$C MAS NMR signals of the above-mentioned product molecules.

The two different pathways for the ethylbenzene disproportionation on zeolites H-Y and H-ZSM-5 are mainly caused by the different pore sizes of these materials [2]. Zeolites show not only characteristic acidities, but also different shape selectivities in hydrocarbon reactions [1]. Investigations of the H/D exchange of the deuterated methyl group during the toluene disproportionation on zeolite H-ZSM-5 showed a scrambling, which indicates a reaction pathway *via* diphenylmethane intermediates [27]. Upon dissolving the zeolite framework in an HF solution after toluene disproportionation on H-ZSM-5, these diphenylmethane species were detected by GC-MS [28]. For xylene disproportionation on H-ZSM-5, however, the larger bimolecular reaction intermediate cannot exist in the small pores and the methoxy-mediated pathway is favored [26]. In the ethylbenzene disproportionation on H-ZSM-5 with significantly smaller pores (*ca.* 0.56 nm) compared to H-Y (*ca.* 0.74 nm), the bulky diphenylethane-type transition state is too large to be formed due to steric restrictions. Therefore and because of the high acid strength of zeolite H-ZSM-5, an ethoxy-mediated intermolecular ethyl group transfer is observed for the ethylbenzene disproportionation on this medium-pore material. But the above-mentioned pathway requires a higher reaction temperature in comparison with the diphenylmethane intermediated route.

### 4.2. Mechanisms of coke formation on zeolites

Upon heating of ethylbenzene-loaded zeolites H-Y and H-ZSM-5 at the reaction temperatures of 533 to 623 K (Figs. 3 and 4), the ethyl cations or ethylene molecules produced after dealkylation of ethylbenzene preferentially form oligomeric species rather than directly transfer to aromatic compounds. With increasing reaction temperature, these oligomeric species are involved in further reactions, which results in increasing $^{13}$C NMR signals of aromatic compounds at 129 ppm and the formation of ethane, propane, toluene and butane. This finding indicates that the aromatic compounds may be produced by the conversion of oligomeric species. The proposed pathway is shown in Scheme 4. Oligomeric cations originating from oligomeric alkoxy groups are transferred into cyclohexanyl cations after six-ring closure [1]. According to the aromatization mechanism of alicyclic hydrocarbons [29], this catalytic reaction involves a series of deprotonation and hydride transfer

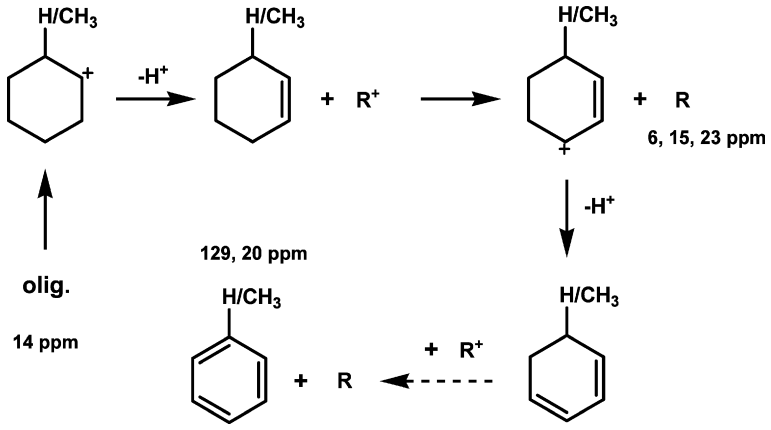


Scheme 4.

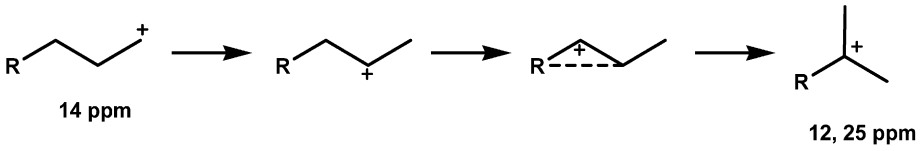


Scheme 5.

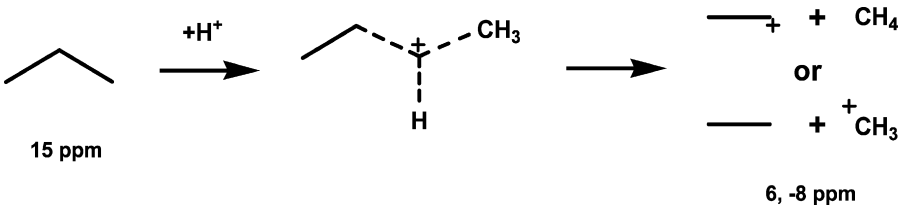


Scheme 6.

steps. In this reaction, cyclohexene species are firstly produced after deprotonation. Subsequently, these cyclohexene species contact alkylcarbenium ions to form cyclohexenyl cations and alkanes by the intermolecular hydride transfer. The alkylcarbenium ions are mainly $C_3$ and $C_4$ hydrocarbon cations, which are also decomposed from oligomeric species. Repetition of these catalytic reactions results in the formation of aromatic compounds and alkanes. Therefore, the increasing signals of aromatic compounds at 129 ppm, butane at 23 ppm, and propane at 15 ppm were observed in the $^{13}C$ MAS NMR spectra shown in Figs. 3 and 4. Overall, the generation of alkylcarbenium ions or alkenes and further intermolecular hydride transfer reactions by them initiate the coke formation and the formation of small alkanes.

At reaction temperatures of 533 to 623 K, the $^{13}C$ MAS NMR spectra of the ethylbenzene conversion on zeolite H-Y consist of two additional signals at 12 and 25 ppm (Fig. 3), which were not observed for this reaction on H-ZSM-5 (Fig. 4). Zeolite H-Y with supercages has more space for the formation of large intermediates of hydrocarbon reactions than the medium-pore zeolite H-ZSM-5. This also effects the isomerization of hydrocarbons on zeolite H-Y. As shown in Scheme 5, skeletal isomerization of oligomeric cations occurs, which leads to iso-alkylcarbenium ions. These carbenium ions can abstract hydrides from other alkanes and transfer to iso-alkanes, which may result in the two new $^{13}C$ MAS NMR signals at 12 and 25 ppm in Fig. 3.

Upon increasing the reaction temperature from 623 to 723 K, the $^{13}C$ MAS NMR signal of methane at −8 ppm starts to appear in the spectra of both zeolites H-Y and H-ZSM-5 (Figs. 3 and 4). With raising temperature, the intensities of the signals of ethane at 6 ppm and methane at −8 ppm increase, which is accompanied by a decrease of the signal of propane at 15 ppm. This finding indicates that the propane is cracked into ethane and methane *via* a protolytic cracking (Scheme 6) on the Brønsted acidic zeolites. The protolytic cracking is favored at high reaction temperatures, which always results in the formation of $C_1$ and $C_2$ products [29]. When the reaction temperature is increased to 723 K for zeolite H-ZSM-5, deep protolytic cracking occurs and more methane molecules are produced (increasing signal at −8 ppm). In the present work, zeolite H-ZSM-5 showed the higher activity in the protolytic cracking of alkanes in comparison with zeolite H-Y. Propane started to be cracked at 623 K on zeolite H-ZSM-5, but at 673 K on zeolite H-Y. Ethane was obviously cracked at 723 K on zeolite H-ZSM-5, but no cracking of ethane was observed at the same temperature on zeolite H-Y. In the monomolecular cracking of propane on zeolites H-ZSM-5, H-MOR, and H-BEA, the higher intrinsic rate constant was obtained for zeolite H-ZSM-5 due to entropic effects [25]. Therefore, higher reactivity of H-ZSM-5 for protolytic cracking in present work is caused by its strong Brønsted acid sites and small pores.

As described before, the conversion of oligomeric species and the intermolecular hydride transfer initiate the coke formation on zeolites at reaction temperatures higher than 533 K. The $^{13}C$ MAS NMR spectra shown in Figs. 4–6 indicate that the amount of coke deposits on zeolite H-ZSM-5 is larger than that on zeolite H-Y. Generally, hydrocarbon reactions on strongly acidic catalysts is accompanied by a high coke formation [1], which may be the most important reason for the larger amount of aromatic deposits on zeolite H-ZSM-5. An effect of the concentration of Brønsted acid sites on the coke formation can be excluded, since for zeolite H-ZSM-5 (0.42 mmol/g) a much smaller concentration of accessible SiOHAl groups than for zeolite H-Y (1.72 mmol/g) was determined. Hence, the concentration of Brønsted acid sites on zeolite H-Y is 4

times higher than that on zeolite H-ZSM-5. The catalytic reaction on zeolite catalysts with a large concentration of acidic hydroxyl protons will promote the transformation of soft coke species and further cracking of them, which may be the reason for the smaller amount of coke deposits on zeolite H-Y than on zeolite H-ZSM-5.

## 5. Conclusions

Zeolites are important catalysts for industrial applications due to their acidic properties and well-defined pore shapes. The *in situ* MAS NMR experiments in the present work provided spectroscopic evidence for understanding the catalytic behavior of the ethylbenzene conversion and the coke formation on Brønsted acidic zeolites. This study shows that not only the acidity, but also the pore size of zeolite catalysts strongly affects the catalytic behavior. Medium-pore zeolite H-ZSM-5 (*ca*. 0.56 nm) and large-pore zeolite H-Y (*ca*. 0.74 nm) with Brønsted acid sites of different acid strength were utilized in this work. $^{13}$C MAS NMR spectroscopic investigations of zeolites H-Y and H-ZSM-5 loaded with ethyl[$\alpha$-$^{13}$C]benzene as reactant and upon heating at different temperatures up to 723 K were performed.

The experiments showed that first diethylbenzene is produced on zeolite H-Y at 453 K. On the stronger acidic zeolite H-ZSM-5, however, ethylbenzene conversion starts at the higher reaction temperature of 503 K. This behavior is caused by the transition state shape selectivity of the zeolites under study [30]: the bulky diphenylethane-type transition state is generated on the large-pore zeolite H-Y and results in an ethylbenzene transalkylation at low temperature, while ethylbenzene dealkylation and realkylation occurs on the medium-pore zeolite H-ZSM-5 at significantly higher reaction temperatures. In the latter case, dealkylated ethyl cations are deprotonated to ethylene and involved in oligomerization and other side-reactions. Therefore, ethylbenzene disproportionation on acidic large-pore zeolites attracts much interest due to the energy saving (low reaction temperatures) and high selectivity (no side-reactions) properties of these reaction systems.

Different pore sizes of zeolites cause not only the above-mentioned shape selectivities in hydrocarbon reactions, but also different catalytic reactivities. Ethylbenzene dealkylation was found to start at 503 K on zeolite H-ZSM-5, but at 573 K on zeolite H-Y. This high reactivity of H-ZSM-5 in the dealkylation promotes the formation of coke deposits. The generated ethyl cations or ethylene molecules are favored to initiate the coke formation by oligomerization rather than direct aromatization. Six-ring closure of decomposed oligomeric species and hydride transfer with carbenium ions result in the formation of aromatics. Furthermore, light alkanes are produced and involved in protolytic cracking. Therefore, the generation of alkylcarbenium ions by dealkylation reactions is the main reason for coke formation, responsible for the rapid deactivation of zeolite H-ZSM-5 in the ethylbenzene disproportionation. At high reaction temperatures, zeolite H-ZSM-5 shows the higher reactivity in the protolytic cracking of light alkanes due to its stronger Brønsted acid sites and smaller pores compared with zeolite H-Y. The latter zeolite, on the other hand, provides supercages for the isomerization of hydrocarbons and the larger concentration of Brønsted acid sites for soft coke transformation and further cracking.

## Acknowledgments

We thank Deutsche Forschungsgemeinschaft and Volkswagen-Stiftung Hannover for financial support.

## References

[1] G. Ertl, H. Knözinger, F. Schüth, J. Weitkamp, Handbook of Heterogeneous Catalysis, VCH, Weinheim, 2008.
[2] D.S. Santilli, J. Catal. 99 (1986) 327.
[3] M. Stöcker, Microporous Mesoporous Mater. 82 (2005) 257.
[4] R.V. Jasara, S.G.T. Bhat, Sep. Sci. Technol. 23 (1988) 945.
[5] A. Streitwieser, L. Reif, J. Am. Chem. Soc. 82 (1960) 5003.
[6] D.A. McCaulay, A.P. Lien, J. Am. Chem. Soc. 75 (1953) 2411.
[7] A.P. Lien, D.A. McCaulay, J. Am. Chem. Soc. 75 (1953) 2407.
[8] H.G. Karge, K. Hatada, Y. Zhang, R. Fiedorow, Zeolites 3 (1983) 13.
[9] H.G. Karge, J. Ladebeck, Z. Sarbak, K. Hatada, Zeolites 2 (1982) 94.
[10] M. Weihe, M. Hunger, M. Breuninger, H.G. Karge, J. Weitkamp, J. Catal. 198 (2001) 256.
[11] U. Weiß, M. Weihe, M. Hunger, H.G. Karge, J. Weitkamp, Stud. Surf. Sci. Catal. 105 (1997) 973.
[12] H.G. Karge, S. Ernst, M. Weihe, U. Weiß, J. Weitkamp, Stud. Surf. Sci. Catal. 84 (1994) 1805.
[13] N. Arsenova, H. Bludau, W.O. Haag, H.G. Karge, Microporous Mesoporous Mater. 23 (1998) 1.
[14] N. Arsenova, H. Bludau, W.O. Haag, H.G. Karge, Microporous Mesoporous Mater. 35–36 (2000) 113.
[15] D.E. De Vos, S. Ernst, C. Perego, C.T. O'Connor, M. Stöcker, Microporous Mesoporous Mater. 56 (2002) 185.
[16] E.E. Wolf, F. Alfani, Catal. Rev. Sci. Eng. 24 (1982) 329.
[17] M. Hunger, J. Weitkamp, Angew. Chem. Int. Ed. 40 (2001) 2954.
[18] J. Huang, Y. Jiang, V.R.R. Marthala, W. Wang, B. Sulikowski, M. Hunger, Microporous Mesoporous Mater. 99 (2007) 86.
[19] A. Philippou, M.W. Anderson, J. Catal. 167 (1997) 266.
[20] W. Wang, J. Jiao, Y. Jiang, S.S. Ray, M. Hunger, ChemPhysChem 6 (2005) 1467.
[21] A.G. Stepanov, M.V. Luzgin, V.N. Romannikov, V.N. Sidelnikov, E.A. Paukshtis, J. Catal. 178 (1998) 466.
[22] J. Huang, Y. Jiang, V.R.R. Marthala, Y.S. Ooi, M. Hunger, ChemPhysChem 9 (2008) 1107.
[23] A. Bhan, E. Iglesia, Acc. Chem. Res. 41 (2008) 559.
[24] A. Pradhan, J. Wu, S. Jong, W. Chen, T. Tsai, S. Liu, Appl. Catal. A 159 (1997) 187.
[25] A. Bhan, R. Gounder, J. Macht, E. Iglesia, J. Catal. 253 (2008) 221.
[26] L.A. Clark, M. Sierka, J. Sauer, J. Am. Chem. Soc. 126 (2004) 936.
[27] Y. Xiong, P.G. Rodewald, C.D. Chang, J. Am. Chem. Soc. 117 (1995) 9427.
[28] S. Svelle, U. Olsbye, K.-P. Lillerud, S. Kolboe, M. Bjørgen, J. Am. Chem. Soc. 128 (2006) 5618.
[29] J.A. Martens, P.A. Jacobs, Stud. Surf. Sci. Catal. 137 (2001) 633.
[30] J. Huang, Y. Jiang, V.R.R. Marthala, M. Hunger, J. Am. Chem. Soc. 130 (2008) 12642.